Magnesium Technology 2011
Edited by: Wim H. Sillekens, Sean R. Agnew, Neale R. Neelameggham, and Suveen N. Mathaudhu
TMS (The Minerals, Metals & Materials Society), 2011

CRYSTAL PLASTICITY MODELING OF PURE MAGNESIUM CONSIDERING VOLUME FRACTION OF DEFORMATION TWINNING

Yuichi Tadano[1]
[1]Saga University; 1 Honjo-machi; Saga 840-8502, Japan

Keywords: Crystal Plasticity, Pure Magnesium, Deformation Twinning, HCP metal.

Abstract

In this study, a novel crystal plasticity model for pure magnesium involving the deformation twinning is presented. The deformation twinning is an important deformation mechanism of magnesium and other HCP metals. The deformation twinning has two important issues: first, the large rotation of crystal lattice caused by twinning occurs. Second, in the crystalline scale, the twinned and untwinned regions may simultaneously exist in a grain. Therefore, a crystal plasticity analysis of magnesium should introduce both of them, and the present framework takes these two key features into account. To represent the second issue, the volume fraction of deformation twinning is considered. This paper provides a framework of crystal plasticity model involving the effect of tensile twinning, and a numerical example is conducted to evaluate the evolution of volume fraction of twinned region. It is shown that the present scheme can describe the mixed state of twinned and untwinned regions. The obtained results suggest that the twinned and untwinned regions simultaneously exist even under the large deformation and the volume fraction of twinned region should be considered.

Introduction

Magnesium has drawn much attention as a structural material, especially in the transportation industry. Magnesium, with a density of 1.74×10^3 kg/m^3, is the lightest of the practical metals, and has excellent specific rigidity and specific strength in comparison with other industrial materials. Therefore, it is expected to be used as the next-generation lightweight material to reduce the weight of products [1]. On the other hand, it has poor formability because of two principal reasons: (1) strong anisotropy in the crystalline scale induced by a hexagonal close-packed (HCP) structure, and (2) direction-dependent c-axis deformation twinning [2]. Understanding the deformation mechanism in the crystalline scale and its effect on the macroscopic scale are important in improving the formability of magnesium.

The mechanical properties of polycrystalline metals are strongly affected by their microstructure such as crystalline aggregates. Most industrial metals have a face-centered cubic (FCC), body-centered cubic (BCC), or HCP structure as the crystal lattice, and pure magnesium exists in HCP form at room temperature. In HCP metals, basal slip $(0001)<11\bar{2}0>$ is generally the most easily activated slip system, because the critical resolved stress is much lower than those of other slip systems. Other slip systems that might be active in plastic deformation of magnesium have been reported: the prismatic slip system $\{10\bar{1}0\}<11\bar{2}0>$ and pyramidal slip systems $\{10\bar{1}1\}<11\bar{2}0>$ and $\{11\bar{2}2\}<11\bar{2}3>$. Another important deformation mechanism of magnesium is twinning due to c-axis tension ($\{10\bar{1}2\}<10\bar{1}1>$ twinning) [2]. In contrast with FCC metals, whose slip systems have identical mechanical properties, each slip system in HCP metals shows significantly different behaviors, causing strong anisotropy in most HCP metals.

Recently, multiscale simulations of crystalline scale structures have been actively studied; one model that can describe the microscale behaviors of metals is the crystal plasticity model. Studies of HCP materials using the crystal plasticity approach were actively reported in the last decade. Dawson and Marin showed the framework of polycrystalline plasticity of HCP metals [3], and many reports on investigation of HCP with the polycrystal plasticity approach followed [4-14]. These studies provided many fruitful results and productive discussions to clarify the essential deformation mechanism of HCP metals.

This study focuses on polycrystalline pure magnesium. The deformation twinning is an important deformation mechanism of magnesium. The deformation twinning has two important issues: first, the large rotation of crystal lattice caused by twinning occurs. Second, in the crystalline scale, twinned and untwinned regions may simultaneously exist in a grain. Therefore, a crystal plasticity analysis of magnesium should introduce both of them. To represent the second issue, the volume fraction of deformation twinning is considered, and the material behavior of a grain is described as mixed state of twinned and untwinned regions. This paper provides a framework of crystal plasticity modeling, and a numerical example is conducted to evaluate the evolution of volume fraction of twinned region.

Formulation

Crystal Plasticity Formulation

This study adopts the crystal plasticity model formulated by Peirce et al. [15] and Asaro and Needleman [16]. The velocity gradient $\mathbf{L}$ is assumed to be decomposed into nonplastic and plastic parts:

$$\mathbf{L} = \mathbf{L}^* + \mathbf{L}^p \tag{1}$$

The plastic part of velocity gradient $\mathbf{L}^p$ is defined by the sum of the slip deformation of all slip systems as

$$\mathbf{L}^p = \sum_{\alpha=1}^{N} \dot{\gamma}^{(\alpha)} \left(\mathbf{s}^{(\alpha)} \otimes \mathbf{m}^{(\alpha)} \right) \tag{2}$$

Here $\mathbf{m}^{(\alpha)}$ and $\mathbf{s}^{(\alpha)}$ are the slip plane normal and slip direction vectors, respectively, $\dot{\gamma}^{(\alpha)}$ is the slip rate, and N is the number of

slip systems. The superscript (α) denotes a specific slip system. The plastic deformation rate tensor $\mathbf{D}^{\mathrm{p}}$ and plastic spin tensor $\mathbf{W}^{\mathrm{p}}$ are given by the symmetric and skew-symmetric parts of $\mathbf{L}^{p}$ as

$$\mathbf{D}^{\mathrm{p}} = \left(\mathbf{L}^{\mathrm{p}} + \mathbf{L}^{pT}\right)/2 = \sum_{\alpha=1}^{\mathrm{N}} \dot{\gamma}^{(\alpha)} \left[\left(\mathbf{s}^{(\alpha)} \otimes \mathbf{m}^{(\alpha)} + \mathbf{m}^{(\alpha)} \otimes \mathbf{s}^{(\alpha)}\right)/2\right] \equiv \sum_{\alpha=1}^{\mathrm{N}} \dot{\gamma}^{(\alpha)} \mathbf{p}^{(\alpha)} \tag{3}$$

$$\mathbf{W}^{\mathrm{p}} = \left(\mathbf{L}^{\mathrm{p}} - \mathbf{L}^{pT}\right)/2 = \sum_{\alpha=1}^{\mathrm{N}} \dot{\gamma}^{(\alpha)} \left[\left(\mathbf{s}^{(\alpha)} \otimes \mathbf{m}^{(\alpha)} - \mathbf{m}^{(\alpha)} \otimes \mathbf{s}^{(\alpha)}\right)/2\right] \equiv \sum_{\alpha=1}^{\mathrm{N}} \dot{\gamma}^{(\alpha)} \mathbf{w}^{(\alpha)} \tag{4}$$

The nonplastic deformation rate tensor $\mathbf{D}^{*}$ and plastic spin tensor $\mathbf{W}^{*}$ are given by

$$\mathbf{D}^{*} = \left(\mathbf{L}^{*} + \mathbf{L}^{*T}\right)/2 \tag{5}$$

$$\mathbf{W}^{*} = \left(\mathbf{L}^{*} - \mathbf{L}^{*T}\right)/2 \tag{6}$$

The elastic constitutive law is

$$\overset{\circ}{\boldsymbol{\sigma}}^{*} = \dot{\boldsymbol{\sigma}} - \mathbf{W}^{*}\boldsymbol{\sigma} + \boldsymbol{\sigma}\mathbf{W}^{*} = \mathbf{C} : \mathbf{D}^{*} \tag{7}$$

Here $\mathbf{C}$ is the fourth-order elastic stiffness tensor, and $\overset{\circ}{\mathbf{A}}$ denotes the Jaumann derivative of $\mathbf{A}$. From Eqs. (5) and (7), and the additive decompositions of the deformation velocity and the spin, $\mathbf{D} = \mathbf{D}^{*} + \mathbf{D}^{\mathrm{p}}$ and $\mathbf{W} = \mathbf{W}^{*} + \mathbf{W}^{p}$ respectively, the following relationship is obtained:

$$\overset{\circ}{\boldsymbol{\sigma}} = \mathbf{C} : \mathbf{D} - \sum_{\alpha=1}^{N} \dot{\gamma}^{(\alpha)} \left[\mathbf{C} : \mathbf{p}^{(\alpha)} + \mathbf{w}^{(\alpha)}\boldsymbol{\sigma} - \boldsymbol{\sigma}\mathbf{w}^{(\alpha)}\right] \tag{8}$$

The changes in the direction of $\mathbf{m}^{(\alpha)}$ and $\mathbf{s}^{(\alpha)}$ caused by the rotation of the crystal lattice are calculated by the following equations:

$$\dot{\mathbf{m}}^{(\alpha)} = \mathbf{W}^{*} \cdot \mathbf{m}^{(\alpha)} \tag{9}$$

$$\dot{\mathbf{s}}^{(\alpha)} = \mathbf{W}^{*} \cdot \mathbf{s}^{(\alpha)} \tag{10}$$

The evolution equation of the slip rate $\dot{\gamma}^{(\alpha)}$ is assumed as the rate dependent form

$$\dot{\gamma}^{(\alpha)} = \dot{\gamma}_0 \operatorname{sgn}\left(\tau^{(\alpha)}\right) \left|\frac{\tau^{(\alpha)}}{g^{(\alpha)}}\right|^{1/m} \tag{11}$$

Here $\tau^{(\alpha)}$ is the resolved shear stress obtained by $\tau^{(\alpha)} = \mathbf{s} \cdot \boldsymbol{\sigma}\mathbf{m}$. $\operatorname{sgn}(x) = 1$ if $x \geq 0$ and $\operatorname{sgn}(x) = -1$ if $x < 0$; m and $\dot{\gamma}_0$ are the slip rate sensitivity parameter and the reference strain rate, respectively, and $g^{(\alpha)}$ is the reference slip resistance, which generally depends on both the slip system and the loading history; the evolution equation of $g^{(\alpha)}$ is given as

$$\dot{g}^{(\alpha)} = \sum_{\beta} h_{\alpha\beta} \dot{\gamma}^{(\beta)} \tag{12}$$

Here the matrix $h_{\alpha\beta}$ is the interaction between slip systems, given as

$$h_{\alpha\beta} = \begin{cases} h(\gamma_{\mathrm{a}}) & (\alpha = \beta) \\ q_{\alpha\beta} h(\gamma_{\mathrm{a}}) & (\alpha \neq \beta) \end{cases} \tag{13}$$

$$\gamma_{\mathrm{a}} = \sum_{\alpha} \int_0^t \left|\dot{\gamma}^{(\alpha)}\right| d\tau \tag{14}$$

$q_{\alpha\beta}$ and $h(\gamma_{\mathrm{a}})$ are the matrices describing the latent hardening and the characteristic hardening function, respectively, and their concrete forms are described in the following section. In addition, the rate tangent modulus method [15] is used for numerical integration of the constitutive equation.

Modeling of Slip Deformation

This study focused on pure magnesium at room temperature, whose crystal lattice is an HCP structure. The slip systems considered in this study are illustrated in Figure 1 and Table I. The pyramidal slip system $\{10\bar{1}1\} <11\bar{2}0>$ is also an active

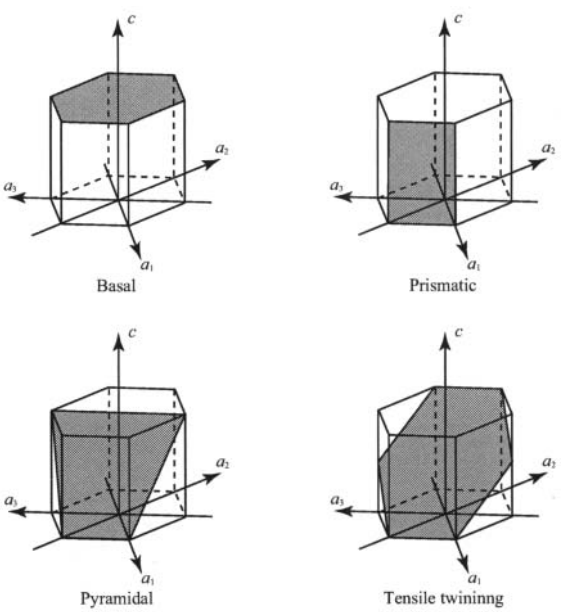

Figure 1. Slip and twining systems in the present analysis.

Table I. Slip and twin systems of HCP crystal.

	Number of Slip Systems	Slip Plane	Slip Direction
Basal	3	(0001)	$<11\bar{2}0>$
Prismatic	3	$\{10\bar{1}0\}$	$<11\bar{2}0>$
Pyramidal	6	$\{11\bar{2}2\}$	$<11\bar{2}\bar{3}>$
Tensile Twin	6	$\{10\bar{1}2\}$	$<10\bar{1}1>$

system in pure magnesium. However, it is neglected in the present study because it can be represented by a superposition of the basal $(0001)<11\bar{2}0>$ system and prismatic system $\{10\bar{1}0\}<11\bar{2}0>$ [7]. Therefore, 12 slip systems and 6 twinning systems are considered here.

On the basis of the experimental results of Kelly and Hosford [17,18], Graff et al. established the following strain hardening laws for pure magnesium [7]:
Linear hardening for a basal system

$$h(\gamma_a) = h_0 \tag{15}$$

Voce hardening for prismatic and pyramidal systems

$$h(\gamma_a) = h_0\left(1-\frac{\tau_0}{\tau_\infty}\right)\exp\left(-\frac{h_0\gamma_a}{\tau_\infty}\right) \tag{16}$$

In this framework, the deformation twinning is taken into account as a slip-like deformation, which can occur only in the tension direction, while general slip can occur in both directions of slip orientation. No reorientation after the saturation of twinning is considered. Therefore, this study takes the lattice rotation caused by the deformation twinning into account as the following manner.

Modeling of Deformation Twinning

If the deformation twinning occurs on a specified twinning plane, the crystal lattice in the twinned region takes the mirrored configuration of the original crystal lattice. The geometrical relation between twinned and untwined regions is expressed with an orthogonal tensor $\mathbf{T}^{\text{twin}}$.

$$\tilde{\mathbf{m}}^{(\alpha)} = \mathbf{T}^{\text{twin}} \cdot \mathbf{m}^{(\alpha)} \tag{17}$$
$$\tilde{\mathbf{s}}^{(\alpha)} = \mathbf{T}^{\text{twin}} \cdot \mathbf{s}^{(\alpha)} \tag{18}$$
$$\mathbf{T}^{\text{twin}} \equiv \mathbf{I} - 2\mathbf{m}^{\text{twin}} \otimes \mathbf{m}^{\text{twin}} \tag{19}$$

Here $\mathbf{m}^{\text{twin}}$ is the vector normal to the twinning plane. $\mathbf{m}^{(\alpha)}$ and $\mathbf{s}^{(\alpha)}$ are the normal to the slip plane and the slip direction vectors in the untwinned region, and $\tilde{\mathbf{m}}^{(\alpha)}$ and $\tilde{\mathbf{s}}^{(\alpha)}$ are those in the twinned region. The norm of each vector is unit. $\mathbf{I}$ denotes the second order unit tensor.

In this study, it is assumed that twinned and untwinned regions simultaneously exist in a material point, and f denotes the volume fraction of the twinned region. After the classical Taylor assumption, the twinned and untwinned region in a material point considered to be subjected a same strain.

$$\mathbf{L}^{\text{parent}} = \mathbf{L}^{\text{twin}} = \mathbf{L}^0 \tag{20}$$

The superscripts parent and twin indicate the untwinned and twined regions, respectively, and $\mathbf{L}^0$ is the macroscopic velocity gradient tensor. In this framework, the twinned and untwinned regions have different stress; therefore the macroscopic stress is defined as the volume average with the volume fraction f

$$\bar{\boldsymbol{\sigma}} = (1-f)\boldsymbol{\sigma}^{\text{parent}} + f\boldsymbol{\sigma}^{\text{twin}} \tag{21}$$

In the same way, the macroscopic constitutive tensor $\bar{\mathbf{C}}$ is give as

$$\bar{\mathbf{C}} = (1-f)\mathbf{C}^{\text{parent}} + f\mathbf{C}^{\text{twin}} \tag{22}$$

The proposed model presents the continuous transition of material properties with respect to deformation twinning.

Numerical results

Analysis Condition

The material parameters for the hardening laws and the components of the latent hardening matrix $q_{\alpha\beta}$ in Eq. (13) are shown in Tables II and III. Graff et al. determined these parameters by fitting simulation results to the channel-die compression tests of single crystal and polycrystal magnesium specimens [7]. In this study, most of parameters are identical as Graff's one; however, τ_0 for the basal slip system is modified to represent the material behaviors after deformation twinning more precisely. Young's modulus, Poisson's ratio, and m and $\dot{\gamma}_0$ in Eq. (11) are set to 45 [GPa], 0.3 [-], 0.02 [-], and 0.001 [s], respectively.

Table II. Material parameters for strain hardening law.

	Basal	Prismatic	Pyramidal
τ_0 / MPa	1	20	40
τ_∞ / MPa	---	150	260
h_0 / MPa	100	7500	7500

Table III. Components of the latent hardening matrix.

α	β			
	Basal	Prismatic	Pyramidal	Twin
Basal	0.2	0.5	0.5	0.5
Prismatic	0.2	0.2	0.2	0.5
Pyramidal	1.0	1.0	0.2	0.25
Twin	1.0	1.0	0.2	0.25

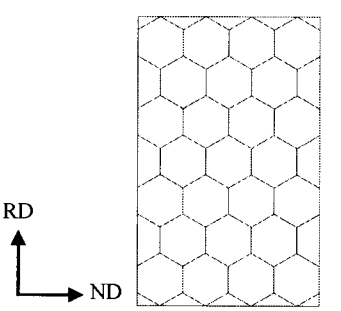

Figure 2. Initial configuration.

The analysis is conducted under the plane strain condition, i.e., $L_{33} = L_{23} = L_{32} = L_{31} = L_{13} = 0$, and the evolution of the volume fraction of twinned region is evaluated. The analysis model of polycrystal is shown in Figure 2. This model is divided by triangular finite elements and the number of finite elements is about 70,000. Note that the three dimensional configuration of crystal lattice is taken into account although the analysis condition is the plane strain. The top and bottom edges are the shear free condition and a compression of 10% nominal strain along RD direction is subjected. Each crystal grain has different initial orientation. A texture similar as the rolled material (rolled texture) and a texture with randomly distributed orientation (random texture) are considered as the initial crystal orientation.

Evolution of Twinned Region

Figure 3 shows the distribution of twinned region at 5% and 10% nominal strain. In case of the rolled texture, each crystal grain has the orientation whose Schmidt factor of a twinning system takes the highest value; therefore, the deformation twinning occurs in several grains even in the case of 5% nominal strain. Almost all material points in some grains are twinned, while only a part of material points are twinned in some grains. When the nominal strain is 10%, the twinned region expands; however, some grains remain to be not twinned. In case of the random textures, a number of twinned grains is fewer than the rolled texture because several grains have orientation hard to occur the deformation twinning. If a specimen is a single crystal, it is expected that all material points are twinned at the same time. However, the present results show that twinned and untwinned regions may exist in the same grain. This tendency is caused by the inhomogeneous deformation due to the constraint between grains in the polycrystalline specimen. Note that the obtained results qualitatively agree with the experimental observations of polycrystalline magnesium [19, 20].

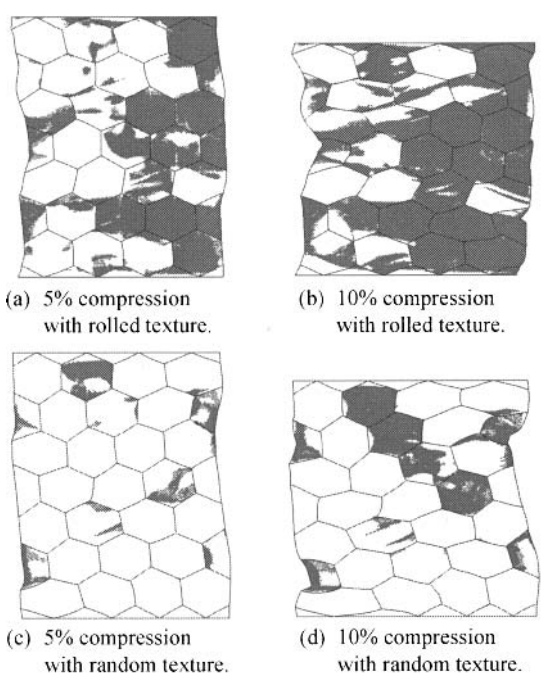

(a) 5% compression with rolled texture.
(b) 10% compression with rolled texture.
(c) 5% compression with random texture.
(d) 10% compression with random texture.

Figure 3. Distributions of twinned region.

The evolution of volume fraction of twinned region is indicated in Figure 4. In case of the rolled texture, the deformation twinning occurs at about 2% nominal strain. In more than half of grains, the volume fraction reaches 100%, i.e., all material points are twinned. On the other hand, the volume fraction converges less than 100% value in some grains. In case of the random texture, the onset of

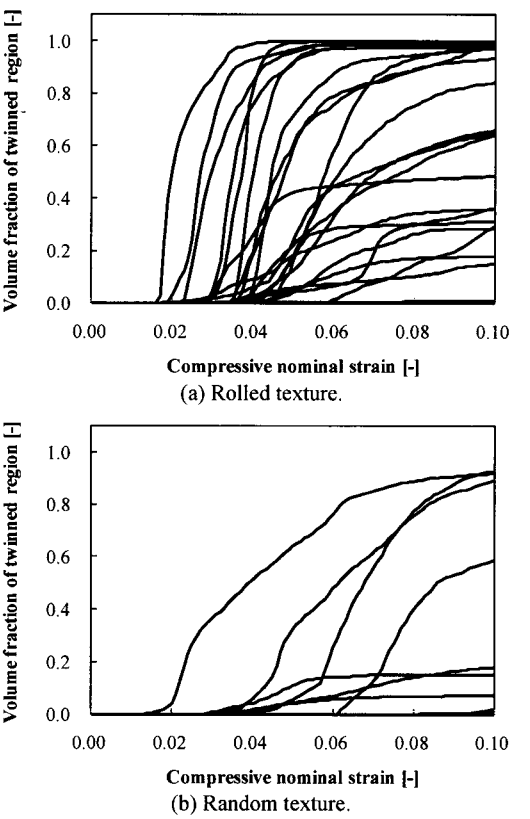

(a) Rolled texture.

(b) Random texture.

Figure 4. Evolution of volume fraction of twinned region.

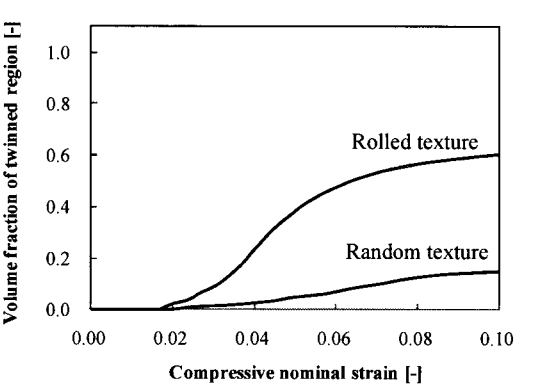

Figure 5. Evolution of volume fraction of twinned region with respect to whole volume of specimen.

deformation twinning delayed than the rolled texture, and the number of twinned grains is fewer; however, the qualitative tendency is similar as the rolled texture. Finally, the volume fraction of twinned region with respect to the whole volume of specimen is shown in Figure 5. The onset of twinning arises at about 2% nominal strain in both cases. At 10% nominal strain, the volume fraction reaches 60% in case of the rolled texture while the fraction is about 15% in case of the random texture. The present results suggest that the twinned and untwinned regions simultaneously exist even under the large deformation, and the volume fraction of twinned region should be considered to develop a constitutive model of polycrystalline pure magnesium.

Concluding Remarks

In this study, a novel crystal plasticity model for pure magnesium involving the deformation twinning is presented. The volume fraction of deformation twinning is considered, and a material behavior of a grain is described as mixed state of twinned and untwinned regions. A numerical example is conducted to evaluate the evolution of volume fraction of twinned region. The obtained results suggest that the twinned and untwinned regions simultaneously exist even under the large deformation, and the volume fraction of twinned region should be considered.

References

1. H.E. Friedrich and B.L. Mordike, *Magnesium technology, metallurgy, design data, applications*, Springer, Berlin, 2006.
2. F.H. Hosford, *Mechanical behavior of materials*, Cambridge University Press, New York, 2005.
3. P.R. Dawson and E.B. Marin, "Computational mechanics for metal deformation processes using polycrystal plasticity," *Adv. Appl. Mech.*, 34 (1998), 77-169.
4. A. Staroselsky and L. Anand, "A constitutive model for hcp materials deforming by slip and twinning: application to magnesium alloy AZ31B," *Int. J. Plasticity*, 19 (2003), 1843-1864.
5. S.R. Agnew et al., "Texture evolution of five wrought magnesium alloys during route A equal channel angular extrusion: Experiments and simulations," *Acta Mater.*, 53 (2005), 3135-3146.
6. S.R. Agnew and O. Duygulu, "Plastic anisotropy and the role of non-basal slip in magnesium alloy AZ31B," *Int. J. Plasticity*, 21 (2005), 1161-1193.
7 S. Graff, W. Brocks, and D. Steglich, "Yielding of magnesium: From single crystal to polycrystalline aggregates," *Int. J. Plasticity*, 23 (2007), 1957-1978.
8. B. Beausir, L.S. Tóth, and K.W. Neale, "Ideal orientations and persistence characteristics of hexagonal close packed crystals in simple shear," *Acta Mater.*, 55 (2007), 2695-2705.
9. B. Beausir et al., "Analysis of texture evolution in magnesium during equal channel angular extrusion," *Acta Mater.*, 56 (2008), 200-214.
10. A. Jain et al., "Grain size effects on the tensile properties and deformation mechanisms of a magnesium alloy, AZ31B, sheet," *Mater. Sci. Eng.*, A 486 (2008), 545-555.
11. G. Proust et al., "Modeling the effect of twinning and detwinning during strain-path changes of magnesium alloy AZ31," *Int. J. Plasticity*, 25 (2009), 861-880.
12. C.J. Neil and S.R. Agnew, "Crystal plasticity-based forming limit prediction for non-cubic metals: Application to Mg alloy AZ31B," *Int. J. Plasticity*, 25 (2009), 379-398.
13. Y. Tadano et al., "A polycrystalline analysis of hexagonal metal based on the homogenized method," *Key Eng. Mat.*, 340-341 (2007), 1049–1054.
14. Y. Tadano, "Polycrystalline behavior analysis of pure magnesium by the homogenization method," *Int. J. Mech. Sci.*, 52 (2010), 257-265.
15. D. Peirce, R.J. Asaro, and A. Needleman, "Material rate dependence and localized deformation in crystalline solids," *Acta Metall.*, 31 (1983), 1951-1976.
16. R.J. Asaro and A. Needleman, "Texture development and strain hardening in rate dependent polycrystals," *Acta Metall.*, 33 (1985), 923-953.
17. E.W. Kelley and W.F. Hosford, "Plane-strain compression of magnesium and magnesium alloy crystals," *Trans. Metall. Soc. AIME*, 242 (1968), 5-13.
18. E.W. Kelley and W.F. Hosford, "The deformation characteristics of textured magnesium," *Trans. Metall. Soc. AIME*, 242 (1968), 654-661.
19. L. Jiang et al., "Twinning and texture development in two Mg alloys subjected to loading along three different strain paths," *Acta Mat.*, 55 (2007), 3899-3910.
20. L. Jiang et al., "Influence of $\{10\bar{1}2\}$ extension twinning on the flow behavior of AZ31 Mg alloy," *Mater. Sci. Eng. A*, 445-446 (2007), 302-309.